

Theoretical investigation of magnetoelectric effects in $\text{Ba}_2\text{CoGe}_2\text{O}_7$

Kunihiko Yamauchi^{1,2}, Paolo Barone¹, and Silvia Picozzi¹

1. *Consiglio Nazionale delle Ricerche (CNR-SPIN), 67100 L'Aquila, Italy*

2. *ISIR-SANKEN, Osaka University, 8-1 Mihogaoka, Ibaraki, Osaka, 567-0047, Japan*

(Dated: July 20, 2018)

A joint theoretical approach, combining macroscopic symmetry analysis with microscopic methods (density functional theory and model cluster Hamiltonian), is employed to shed light on magnetoelectricity in $\text{Ba}_2\text{CoGe}_2\text{O}_7$. We show that the recently reported experimental trend of polarization guided by magnetic field (H. Murakami et al., Phys. Rev. Lett. **105**, 137202 (2010)) can be predicted on the basis of phenomenological Landau theory. From the microscopic side, $\text{Ba}_2\text{CoGe}_2\text{O}_7$ emerges as a prototype of a class of magnetoelectrics, where the cross coupling between magnetic and dipolar degrees of freedom needs, as main ingredients, the on-site spin-orbit coupling and the spin-dependent O p - Co d hybridization, along with structural constraints related to the non-centrosymmetric structural symmetry and the peculiar configuration of CoO_4 tetrahedrons.

PACS numbers: Valid PACS appear here

The magnetoelectric (ME) coupling between the magnetic order parameter (M) and the ferroelectric one (P) has been well studied in recent years in the context of *multiferroic* oxides, where two or more primary ferro phases coexist in the same system.[1] Most of the research focused onto the *linear* ME effect, as expressed by the $\alpha_{ij}H_iE_j$ cross-coupling term, and observed, e.g., in the prototypical Cr_2O_3 . [2] Microscopically, the ME effect can be ascribed to i) the inverse Dzyaloshinskii-Moriya mechanism [3] (or the equivalent spin-current mechanism [4]) showing $\mathbf{P} \propto \sum_{ij} \mathbf{e}_{ij} \times (\mathbf{S}_i \times \mathbf{S}_j)$ between neighboring spins connected by a vector \mathbf{e}_{ij} , and ii) the inverse Goodenough-Kanamori (or exchange-striction) mechanism [5] showing $\mathbf{P} \propto \sum_{ij} J_{ij}(\mathbf{S}_i \cdot \mathbf{S}_j)$ with exchange integral J_{ij} . A third mechanism has been recently proposed, namely iii) the spin-dependent p - d hybridization [6, 7], where the spin-orbit-coupling (SOC) ‘‘asymmetrizes’’ the p - d hybridization between the transition metal (TM) and the surrounding ligands, inducing an electric polarization $\mathbf{P} \propto \sum_{ij} (\mathbf{S}_i \cdot \mathbf{e}'_j)^2 \mathbf{e}'_j$, where \mathbf{e}'_j labels the vectors connecting the TM to the ligand ions. Since the third mechanism can concomitantly occur with the first or second one (in non-collinear spin structures), it is in general difficult to identify each of these mechanisms. However, it has been recently reported that the third mechanism can be responsible for the polarization observed in $\text{Ba}_2\text{CoGe}_2\text{O}_7$ (BCGO), where two neighboring Co spins are aligned in an antiferromagnetic (AFM) configuration. Incidentally, we have discussed a related ME mechanism in Fe_3O_4 , where the crystal structure with Cc space group doesn't have inversion symmetry, but the c -glide symmetry prohibits polarization along the y direction.[8] Taking into account SOC and ferrimagnetic spin order, i.e. considering the magnetic group, the symmetry is broken and a small spin-dependent contribution to polarization arises. In this letter, we apply a similar theoretical analysis to BCGO: we first perform a symmetry analysis, then show the DFT results on the ME effect, and further confirm the microscopic mechanisms in a model Hamiltonian approach.

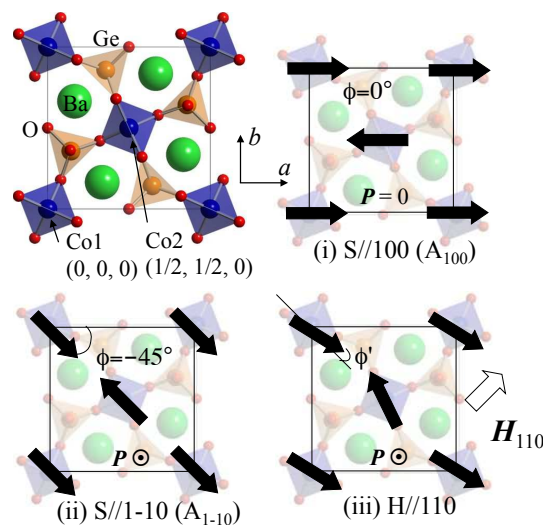


FIG. 1: Crystal structure in the ab plane; Co and Ge ions (both located in O_4 tetrahedron) lie in $c=0$ planes whereas Ba ion lies in $c=1/2$ planes. Co spin configurations: (i), (ii) collinear AFM and (iii) non-collinear spin-canted under applied $\mathbf{H} // 110$.

$\text{Ba}_2\text{CoGe}_2\text{O}_7$ (melilite) shows tetragonal non-centrosymmetric (but non-polar) $P\bar{4}2_1m$ (#113) structure with two Co sites, Co1 at $(0,0,0)$ and Co2 at $(1/2, 1/2, 1/2)$ sites, as shown in Fig. 1. Below $T_N=6.7\text{K}$, the magnetic structure shows collinear AFM spins lying in the ab plane. Experimentally, the electric polarization along the c axis, P_c , is measured even when $\mathbf{H}=0$. [9, 10] Additionally, \mathbf{P} develops finite components along any direction when \mathbf{H} is applied, modulated by the direction and the size of the magnetic field.

Symmetry Analysis. — In order to characterize the peculiar ME effect, we first briefly discuss the group theory analysis and its implications in the framework of Landau theory of phase transitions.[11] In the parent $P\bar{4}2_1m1'$ magnetic space group with eight symmetry operations $\{E, C_{2(z)}, 2S_4, 2C_{2(x,y)}, 2\sigma_d\}$ plus time-reversal ($1'$), the magnetic order leads to a lowered symmetry. We define

TABLE I: Matrices of the generators of space group $P\bar{4}2_1m1'$ in the representations spanned by F , A and P . The group elements denote the identity, π -rotation, $\pi/2$ -rotoinversion, screw $C_{2y}+(\frac{1}{2}\frac{1}{2}0)$ and time-reversal. Labels of irreducible representation (IR) are taken from the ISODISORT program.[12]

	E	C_{2z}	S_4^-	C_{2y}	$1'$	IR
F_a	$\begin{bmatrix} 1 & 0 \\ 0 & 1 \end{bmatrix}$	$\begin{bmatrix} -1 & 0 \\ 0 & -1 \end{bmatrix}$	$\begin{bmatrix} 0 & 1 \\ -1 & 0 \end{bmatrix}$	$\begin{bmatrix} -1 & 0 \\ 0 & 1 \end{bmatrix}$	$\begin{bmatrix} -1 & 0 \\ 0 & -1 \end{bmatrix}$	$m\Gamma_5 E_{1a}^*$
F_b	$\begin{bmatrix} 0 & 1 \\ 1 & 0 \end{bmatrix}$	$\begin{bmatrix} 0 & -1 \\ 1 & 0 \end{bmatrix}$	$\begin{bmatrix} -1 & 0 \\ 0 & 1 \end{bmatrix}$	$\begin{bmatrix} 0 & 1 \\ -1 & 0 \end{bmatrix}$	$\begin{bmatrix} 0 & -1 \\ -1 & 0 \end{bmatrix}$	$m\Gamma_5 E_{1b}^*$
F_c	1	1	1	-1	-1	$m\Gamma_4 A$
A_a	$\begin{bmatrix} 1 & 0 \\ 0 & 1 \end{bmatrix}$	$\begin{bmatrix} -1 & 0 \\ 0 & -1 \end{bmatrix}$	$\begin{bmatrix} 0 & 1 \\ -1 & 0 \end{bmatrix}$	$\begin{bmatrix} 1 & 0 \\ 0 & -1 \end{bmatrix}$	$\begin{bmatrix} -1 & 0 \\ 0 & -1 \end{bmatrix}$	$m\Gamma_5 E_{2b}^*$
A_b	$\begin{bmatrix} 0 & 1 \\ 1 & 0 \end{bmatrix}$	$\begin{bmatrix} 0 & -1 \\ 1 & 0 \end{bmatrix}$	$\begin{bmatrix} -1 & 0 \\ 0 & 1 \end{bmatrix}$	$\begin{bmatrix} 0 & -1 \\ -1 & 0 \end{bmatrix}$	$\begin{bmatrix} 0 & -1 \\ -1 & 0 \end{bmatrix}$	$m\Gamma_5 E_{2a}^*$
A_c	1	1	1	1	-1	$m\Gamma_1 A$
P_a	$\begin{bmatrix} 1 & 0 \\ 0 & 1 \end{bmatrix}$	$\begin{bmatrix} -1 & 0 \\ 0 & -1 \end{bmatrix}$	$\begin{bmatrix} 0 & -1 \\ 1 & 0 \end{bmatrix}$	$\begin{bmatrix} -1 & 0 \\ 0 & 1 \end{bmatrix}$	$\begin{bmatrix} 1 & 0 \\ 0 & 1 \end{bmatrix}$	Γ_5
P_b	$\begin{bmatrix} 0 & 1 \\ 1 & 0 \end{bmatrix}$	$\begin{bmatrix} 0 & -1 \\ 1 & 0 \end{bmatrix}$	$\begin{bmatrix} 1 & 0 \\ 0 & 1 \end{bmatrix}$	$\begin{bmatrix} 0 & 1 \\ -1 & 0 \end{bmatrix}$	$\begin{bmatrix} 0 & 1 \\ -1 & 0 \end{bmatrix}$	Γ_5
P_c	1	1	-1	-1	1	Γ_3

the order parameters $\mathbf{F} = \mathbf{S}_1 + \mathbf{S}_2$ and $\mathbf{A} = \mathbf{S}_1 - \mathbf{S}_2$ as the ferromagnetic (FM) and AFM combination of Co1 and Co2 spins, respectively. Using the transformation rules given in Table I, we express the thermodynamic free energies in terms of all the possible ME coupling terms of the form $\mathbf{P} \cdot \mathbf{M}^2$ which are invariant under symmetry operations:

$$F_{\text{ME}} = c_A P_c A_a A_b + c_F P_c F_a F_b + c_{\text{AF}} P_c (A_a F_a - A_b F_b) + c_1 (P_a A_a F_c - P_b A_b F_c) + c_2 (P_a A_c F_a - P_b A_c F_b), \quad (1)$$

while the dielectric energy is $F_{\text{DE}} = -\mathbf{P}^2/2\chi$, where $c_A, c_F, c_1, c_2, c_{\text{AF}}$ and χ (henceforth set as 1) are constants. \mathbf{P} is then evaluated at the minima of $F = F_{\text{ME}} + F_{\text{DE}}$, reading

$$P_a = c_1 A_a F_c + c_2 A_c F_a, \quad P_b = -c_1 A_b F_c - c_2 A_c F_b, \\ P_c = c_A A_a A_b + c_F F_a F_b + c_{\text{AF}} (A_a F_a - A_b F_b). \quad (2)$$

Note that only the first term of P_c originates purely from the AFM order, explaining the observed spontaneous \mathbf{P} , whereas other components are allowed only in the presence of the FM order parameter.

Hereafter we focus on the P_c behavior assuming a canted AFM configuration under an applied magnetic field, i.e., we first simultaneously counter-clock-wise rotate two antiparallel Co spins in the ab plane with the angle ϕ from the a axis, then we cant spins by an angle ϕ' , as depicted in Fig. 1. Accordingly, we set $\mathbf{S}_1 = S(\cos(\phi + \phi'), \sin(\phi + \phi'), 0)$ and $\mathbf{S}_2 = S(-\cos(\phi - \phi'), -\sin(\phi - \phi'), 0)$, ending up with

$$P_c(\phi) = 2S^2 \sin 2\phi (c_A \cos^2 \phi' - c_F \sin^2 \phi' - c_{\text{AF}} \sin 2\phi') \\ = 2\alpha S^2 \sin 2\phi \cos(2\phi' - \beta), \quad (3)$$

where $\alpha^2 = c_{\text{AF}}^2 + (c_A + c_F)^2/2$ and $\tan \beta = -(c_A + c_F)/2c_{\text{AF}}$. By neglecting the canting angle ϕ' , Eq. (3) perfectly reproduces the experimentally observed dependence of polarization on the spin angle, being $P_c \propto \sin 2\phi$ at $T=2\text{K}$ and $H=1\text{T}$. [10] A spontaneous P_c can be therefore induced in the A_{110} (A_{1-10}) order but not in the A_{100} (A_{010}) one (cfr. Fig. 1). Analogously to the case of magnetite[8], the non-magnetic group lacks the inversion

symmetry, but the symmetries which prohibit P_c (e.g. C_{2y} rotation) are broken by the A_{110} magnetic order. Starting from the A_{110} order, further symmetry reduction occurs by applying an external \mathbf{H} . Indeed, A_{110} order shows $2'_z$ point group, which allows non-zero $\alpha_{13}, \alpha_{23}, \alpha_{31}, \alpha_{32}$ linear ME components[13] in such a way that P_a and P_b can be induced by applying H_z . Finally, Eq. (3) at fixed ϕ gives the simple ϕ' -dependence $P_c(\phi') \propto \alpha \cos(2\phi' - \beta)$, where the phase shift depends on the non-zero c_{AF} coefficient.

DFT analysis — In order to quantitatively confirm the ME behavior and to investigate its microscopic mechanism, we performed DFT calculations using VASP[14] with GGA-PBE potential (we checked our results by using also GGA+ U [15] potential with $U=3$ or 5 eV for Co- d state). Due to the lack of experimental information on structural parameters, we considered the $\text{Ca}_2\text{CoSi}_2\text{O}_7$ structure[16] and optimize it by substituting atoms ($\text{Ca} \leftrightarrow \text{Ba}$, $\text{Si} \leftrightarrow \text{Ge}$) without SOC. The optimized structures shows $a=b=8.28\text{\AA}$ and $c=5.58\text{\AA}$, and the tilting angle of CoO_4 tetrahedron given by $\kappa=23.9^\circ$, consistent with experimental values, $a=b=8.41\text{\AA}$ and $c=5.54\text{\AA}$ [9] and $\kappa=24^\circ$. [10]

TABLE II: Magnetic anisotropy energy (MAE) (meV/Co) obtained by comparing the total energy with different spin directions under SOC and for different values of U in the GGA+ U scheme. Spin and orbital moment (μ_B) are also reported for $S//\langle 100 \rangle$. In the rightmost column we report the calculated P_c ($\mu\text{C}/m^2$) for S (L)/110 with fixed atomic structure.

	$E(100)$	$E(110)$	$E(001)$	S	L	P_c
bare GGA	0	0.00	+0.17	2.53	0.17	12.7
$U=3\text{eV}$	0	0.00	+0.16	2.61	0.17	12.2
$U=5\text{eV}$	0	-0.31	+0.65	2.75	0.24	10.6

In the CoO_4 tetrahedra, the Co^{2+} ion shows orbital-quenched $e_g^{\uparrow} t_{2g}^{\uparrow 3} e_g^{\downarrow} t_{2g}^{\downarrow 0}$ states, which causes a very small magnetic anisotropy, as shown in Table II. The observed magnetically easy ab plane and hard c axis are consistent with experimental report ($S//010$ from Neutron diffraction[17]). The small MAE in the ab plane explains why the spins easily follow an applied \mathbf{H} : even under a small magnetic field, the spins flop to be perpendicular to \mathbf{H} and then cant in order to reduce the Zeeman energy.

Imposing the collinear AFM configuration, we simultaneously rotate the Co spins in the ab plane. We evaluated the ME effect as the change of \mathbf{P} (calculated by Berry phase method [18]) induced by the rotation of \mathbf{M} with respect to the crystalline axes, in the fixed non-polar crystal structure. In Fig. 2 (a) we show P_c as a function of the spin-rotation angle ϕ , consistent with both experiments and the previously discussed Landau analysis, being $P_c \propto \sin 2\phi$. The calculated polarization, which displays a maximum value $P_c = 12.7 \mu\text{C}/m^2$ at A_{1-10} , originates here from a purely electronic contribution via SOC, and is further enhanced when atomic internal coordinates are optimized in the A_{1-10} configuration, as

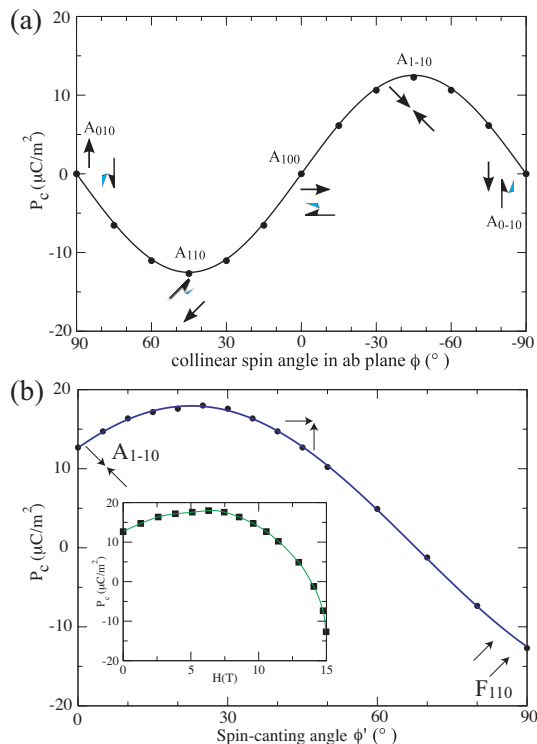


FIG. 2: (a) DFT results for P_c as a function of the **collinear** spin angle ϕ in the ab plane, fitted to $f(\phi) = -a \sin 2\phi$, with $a=12.7$ (solid line). Spin configurations in the ab plane are shown by arrow. (b) DFT results for P_c as a function of the **noncollinear** spin-canting angle ϕ' in the ab plane, fitted to $f(\phi') = a \cos 2(\phi' - b) + c$, with $a=17.9$, $b=22.7$ and $c=0.06$ (solid line). Inset: P_c as a function of magnetic field.

discussed later.

TABLE III: P_c at different canting angle ϕ' , calculated in the fixed non-polar structure (first line) and with optimized internal atomic coordinates (second line). Experimentally, the maximum of P_c is about $120 \mu\text{C}/\text{m}^2$ [10].

P_c ($\mu\text{C}/\text{m}^2$)	$\phi' = 0^\circ$	30°	90°
fixed structure	12.7	17.6	-12.7
opt. structure	39.8	57.7	-38.9

We look then at the spin-canting effect induced by an applied field H_{110} . In Fig. 2 (b) we show the change in P_c induced by artificially canting the spins by an angle ϕ' , starting from the A_{1-10} AFM configuration. In agreement with the Landau theory analysis, P_c evolves as $\cos 2(\phi' - 22.7^\circ) + \text{const.}$, displaying a peak at $\phi' \sim \kappa$. We also evaluate the evolution of P_c as a function of the applied H (cfr. inset in Fig. 2 (b)), assuming the experimentally measured magnetic susceptibility $\chi = M/H_{110} \approx 0.25 \mu\text{B}/\text{T}$ per Co[10]. Although the trend of P shows good agreement with experiments[10], its size is one order of magnitude smaller. This deviation is reduced when the atomic structure is optimized in the canted-AFM configuration, as shown in Table III. This means that ferroelectricity is strongly coupled,

through magnetism, with lattice distortions in a sort of *magnetically-induced piezoelectric effect*. The PH curve—first increasing with H and then decreasing and changing its sign—denotes an atypical ME trend. Although one may assume a non-linear ME coupling coming from high-order terms in the free energy, the nontrivial evolution of P actually arises from the composition of the three $\mathbf{P} \cdot \mathbf{M}^2$ terms appearing in Eq. (1).

Single-site SOC induced ME effect—The microscopic origin of \mathbf{P} in BCGO can be easily explained in terms of a cluster Hamiltonian for a single CoO_4 tetrahedron, which allows to further clarify the role of the local SOC in the spin-dependent p - d hybridization mechanism. Neglecting contributions from the energetically deeper majority-spin states, the Hamiltonian consists of four terms, $H = H_d + H_p + H_{pd} + H_{\text{SOC}}$, where $H_d = \Delta \sum_{\alpha} d_{\alpha}^{\dagger} d_{\alpha}$ and $H_p = \varepsilon_p \sum_{l,\beta} p_{l,\beta}^{\dagger} p_{l,\beta}$ account for the local energies on Co and O sites (with $\varepsilon_p = 0$ the energy reference and $\Delta = \varepsilon_d - \varepsilon_p$), which hybridize through $H_{pd} = \sum_{\alpha,\beta,l} V_{\alpha\beta l} (d_{\alpha}^{\dagger} p_{l,\beta} + h.c.)$. Here α and β refer to the $d = xy, yz, zx, x^2-y^2, 3z^2-r^2$ and $p = x, y, z$ orbitals involved, whereas $l = 1, \dots, 4$ labels the four oxygens surrounding the Co ion, located at $\mathbf{R}_l = (1, 1, -1), (-1, -1, -1), (1, -1, 1)$ and $(-1, 1, 1)$ in the local reference system with Co in the origin. The hybridization matrix $V_{\alpha\beta l}$ depends on the d and p orbitals involved (with σ or π bonding) and on the relative positions of the ions; we adopted the Slater-Koster parametrization[19], assuming $t_{pd\sigma} = 1.3 eV$, $\Delta = 5.5 eV$ [20] and $t_{pd\pi} = -0.45 t_{pd\sigma}$ [21]. The last term is $H_{\text{SOC}} = \lambda \sum_{\alpha,\alpha'} \langle \alpha | L \cdot S | \alpha' \rangle d_{\alpha}^{\dagger} d_{\alpha'}$, where the matrix elements can be expressed as a function of the polar and azimuthal angles (θ, ϕ) defining a local reference for the spin-quantization axis[22]. We assume $\lambda = 0.021 eV$, the free Co ion spin-orbit coupling value. SOC-induced mixing of the local d levels lifts the degeneracies in the e_g and t_{2g} manifolds and implies different hybridizations with the ligand oxygens, that may ultimately induce a local dipole moment. We evaluated

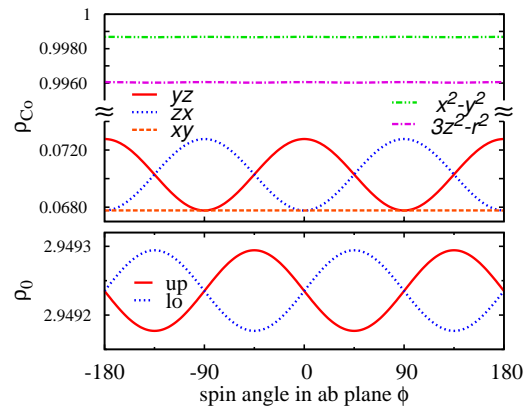


FIG. 3: Model results. (bottom) Electron density of upper- and lower-lying oxygens, ρ_O , in the tetrahedron model as a function of the azimuthal angle ϕ at $\theta = 90^\circ$. (top) Orbital occupancy on Co, $\rho_{\text{Co}}^{\alpha}$, as a function of ϕ .

then the local occupancies as $\rho_{O(l)} = \sum_{\beta} \langle p_{l,\beta}^{\dagger} p_{l,\beta} \rangle$ and $\rho_{Co} = \sum_{\alpha} \langle d_{\alpha}^{\dagger} d_{\alpha} \rangle$ as a function of the azimuthal angle ϕ , i.e. rotating the spin in the ab plane. As shown in Fig. 3, we can distinguish between lower-lying (O_1, O_2) and upper-lying (O_3, O_4) oxygens, with $\rho_{up,lo} \propto \pm \sin(2\phi)$. Then a local dipole $\mathbf{p} = (e/4) \sum_l \rho_{O(l)} \mathbf{R}_l$ may develop only along c , proportional to the charge difference $\Delta\rho_O = \rho_{up} - \rho_{lo}$, i.e. $p_c \propto 2 \sin 2\phi$, in excellent agreement with the predicted functional form $\mathbf{P} \propto \sum_{ij} (\mathbf{S}_i \cdot \mathbf{e}'_j)^2 \mathbf{e}'_j$ [6, 7, 10]. Furthermore, we can estimate the d -orbital mixing on the Co site by looking at the orbital occupancies, shown in Fig. 3. Even if the two occupied states have prevalent $d_{x^2-y^2}, d_{3z^2-r^2}$ characters, a small mixing occurs via SOC with (mostly) d_{yz}, d_{zx} orbitals, being $\rho_{yz} \propto \cos^2 \phi, \rho_{zx} \propto \sin^2 \phi$, i.e. the most occupied is the one perpendicular to the spin-quantization axis.

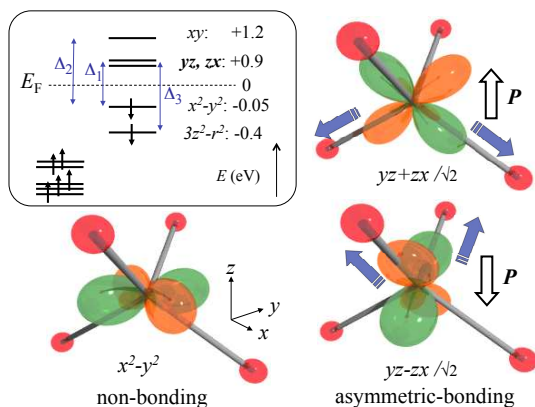


FIG. 4: Bonding nature of d -orbital in O_4 tetrahedron and induced local polarization. Via SOC, asymmetrically bonded orbital states are mixed with non-bonding occupied states. Inset: DFT-calculated energy levels of orbital states. Possible SOC mixing in minority spin states are shown with energy difference Δ_i .

TABLE IV: DFT-calculated $3d$ orbital-decomposed occupancy (in percentage, with spin states summed up) with different SOC enhancement factors λ (0=without SOC, $\times 1$ =with standard SOC, and $\times 10$ =with the SOC term 10 times artificially enhanced) for different \mathbf{S} directions in local xyz frame.

λ	\mathbf{M}	xy	yz	zx	$3z^2-r^2$	x^2-y^2
0	-	50.0	50.0	50.0	100.0	100.0
$\times 1$	$\mathbf{S} // \mathbf{x}$	50.0	50.2	50.0	99.9	99.9
$\times 1$	$\mathbf{S} // \mathbf{y}$	50.0	50.0	50.2	99.9	99.9
$\times 10$	$\mathbf{S} // \mathbf{x}$	49.5	61.7	49.7	92.8	96.3
$\times 10$	$\mathbf{S} // \mathbf{y}$	49.5	49.7	61.7	92.8	96.3

These findings are in excellent agreement with DFT calculations, as shown in Fig. 4 and in Table IV, where the hierarchy of d -orbital occupancies at selected values of the spin direction is confirmed. Such a mixing of local d -levels nicely explains why p_c size is maximum at $\phi = \pm 45^\circ$, when the Co spin is parallel either to the upper- or to the lower-lying oxygen bond; indeed, as pictorially shown in Fig. 4, the composition of yz and zx

orbitals has an asymmetric bonding nature in the tetrahedron, i. e. non-bonding with upper ligands and bonding with lower ligands or vice versa.

We can further estimate from our model the P_c dependence on the spin angle in the system by considering two CoO_4 tetrahedra tilted by κ . In the AFM collinear configuration we find $P_c \propto p_{c1}(\phi + \kappa) + p_{c2}(\phi + \pi - \kappa) = 2 \cos \kappa \sin 2\phi$. Analogously, in order to mimick the effect of the external H_{110} , we can define the canting angles as $\phi'_1 = \phi + \kappa - \pi/4$ and $\phi'_2 = -\phi + \kappa + 3\pi/4$, finding $P_c(\phi') \propto \cos 2(\phi' - \kappa)$, in excellent agreement with experiments and DFT results.

Conclusions —

We shed light on the mechanism underlying peculiar magnetoelectric effects in $Ba_2CoGe_2O_7$, by combining different theoretical approaches and explicitly taking into account the microscopic atomic arrangement and symmetries of the compound. Our Landau phenomenological theory shows that: i) On top of non-centrosymmetric non-polar $P\bar{4}2_1m$ symmetry in the non-magnetic crystal structure, a collinear antiferromagnetic spin configuration with in-plane spins allows an electric polarization along the z axis. ii) Upon applying an external magnetic field, the induced non-collinear spin-canting well reproduces the experimentally observed peculiar trend of polarization related to the tilting angle between CoO_4 tetrahedrons. In order to have quantitative estimates, we perform relativistic ab-initio calculations and highlight the delicate interplay between orbital occupation and local magnetic anisotropy, resulting in an excellent match with available experiments. Furthermore, as a proof that the microscopic origin of magnetoelectricity is based on two relevant ingredients (i.e. the anisotropic p - d hybridization between Co and O states and the on-site spin-orbit coupling), we built a realistic tight-binding model, taking into account CoO_4 tetrahedron and the crystal field splitting, that is sufficient to nicely explain magnetoelectric effects and put forward $Ba_2CoGe_2O_7$ as a prototype of the class of materials where the interplay between magnetism and ferroelectricity is based on spin-dependent $p-d$ hybridization, as recently suggested in the literatures based on two-ion cluster model.[10, 23]

During completion of the work, we became aware of a similar symmetry analysis [24] performed for BCGO by Toledano *et al.*. However, their focus is on toroidal moments, whereas ours is on the combination between single-ion anisotropy and $p-d$ hybridization (derived from density functional and tight-binding models) as main microscopic mechanism driving magnetoelectricity.

Acknowledgments

Authors thank Y. Tokura and J. Manuel Perez-Mato for fruitful discussions. The research leading to these results has received funding from the EU Seventh Framework Programme (FP7/2007-2013) under the ERC grant

agreement n. 203523-BISMUTH. Computational support from Caspur Supercomputing Center (Rome) is

gratefully acknowledged.

-
- [1] M. Fiebig, J. Phys. D: Appl. Phys. **38** R123 (2005).
 [2] J. Íñiguez, Phys. Rev. Lett. **101**, 117201 (2008).
 [3] I. A. Sergienko and E. Dagotto, Phys. Rev. B **73**, 094434 (2006).
 [4] H. Katsura, N. Nagaosa, and A. V. Balatsky, Phys. Rev. Lett. **95**, 057205 (2005).
 [5] T. Arima et al., Phys. Rev. Lett. **96**, 097202 (2006).
 [6] T. Arima, J. Phys. Soc. Jpn. **76**, 073702 (2007).
 [7] C. Jia, et. al., Phys. Rev. B **76**, 144424 (2007).
 [8] K. Yamauchi and S. Picozzi, arXiv:1010.1105.
 [9] H. T. Yi et al, Appl. Phys. Lett. **92**, 212904 (2008).
 [10] H. Murakawa et al. Phys. Rev. Lett. **105**, 137202 (2010).
 [11] L. D. Landau and E. M. Lifshitz, Statistical Physics, Part I (Pergamon Press, Oxford, 1980).
 [12] B. J. Campbell et al, J. Appl. Cryst. **39**, 607 (2006).
 [13] International Tables for Crystallography, Vol. D, Physical Properties of crystals, Edited by A. Authier, Kluwer Academic Publishers, 2003
 [14] G. Kresse and J. Furthmüller, Phys. Rev. B **54**, 11169 (1996).
 [15] V. I. Anisimov, F. Aryasetiawan and A. I. Lichtenstein, J. Phys.: Cond. Mat. **9**, 767 (1997).
 [16] K. Hagiya and M. Ohmasa, Acta Cryst. **B49**, 172 (1993).
 [17] A. Zheludev et al, Phys. Rev. B **68**, 024428 (2003).
 [18] R.D.King-Smith and D.Vanderbilt, Phys. Rev. B **47**, 1651 (1993); R. Resta, Rev. Mod. Phys **66**, 899 (1994).
 [19] J. C. Slater and G. F. Koster, Phys. Rev. **94**, 1498 (1954).
 [20] J. van Elp and A. Tanaka, Phys. Rev. B **60**, 5331 (1999).
 [21] W. A. Harrison, *Electronic Structure and the Properties of Solids* (Freeman, San Francisco, 1980).
 [22] H. Takayama, K bohnens and P. Fulde, Phys. Rev. B **14**, 2287 (1976).
 [23] S. Miyahara and N. Furukawa arXiv:1101.3679v1.
 [24] P. Toledano, D. D. Khalyavin and L. C. Chapon, arXiv:1012.0785.v1